European Conference on Computational Fluid Dynamics
ECCOMAS CFD 2006
P. Wesseling, E. Oñate and J. Périaux (Eds)

SOLUTION OF COMPRESSIBLE FLOW WITH ALL MACH NUMBERS

Miloslav Feistauer* **and Václav Kučera†**

*Charles University Prague, Faculty of Mathematics and Physics
Sokolovská 83, 186 75 Praha 8, Czech Republic
e-mail: feist@karlin.mff.cuni.cz
web page: http://www.karlin.mff.cuni.cz/ feist/
†Charles University Prague, Faculty of Mathematics and Physics
Sokolovská 83, 186 75 Praha 8, Czech Republic
e-mail: vaclav.kucera@email.cz

Key words: Compressible inviscid flow, Discontinuous Galerkin method, Semi-implicit scheme, Wide range of Mach numbers, Boundary conditions, Shock capturing, Accuracy of the method

Abstract. *This work is concerned with the numerical solution of an inviscid compressible flow. Our goal is to develop a sufficiently accurate and robust method allowing the solution of problems with a wide range of Mach numbers. The main ingredients are the discontinuous Galerkin finite element method (DGFEM), semi-implicit time stepping, special treatment of transparent boundary conditions and a suitable limiting procedure near discontinuities. Numerical experiments show the robustness of the method.*

1 INTRODUCTION

In the numerical solution of compressible flow, it is necessary to overcome a number of obstacles. Let us mention the necessity to resolve accurately shock waves, contact discontinuities and (in viscous flow) boundary layers, wakes and their interaction. Some of these phenomena are connected with the simulation of high speed flow with high Mach numbers. However, it appears that the solution of low Mach number flow is also rather difficult. This is caused by the stiff behaviour of numerical schemes and acoustic phenomena appearing in low Mach number flows at incompressible limit. In this case, standard finite volume schemes fail. This led to the development of special finite volume techniques allowing the simulation of compressible flow at incompressible limit, which is based on modifications of the Euler or Navier-Stokes equations. (See, e. g. [13], [16], [19], Chapter 14, or [15], Chapter 5.)

Here we are concerned with the development of an efficient, robust and accurate method allowing the solution of compressible flow with a wide range of the Mach number without any modification of the governing equations. This technique is based on the *discontinuous*

Galerkin finite element method (DGFEM), which can be considered as a generalization of the finite volume as well as finite element methods, using advantages of both these techniques. It employs piecewise polynomial approximations without any requirement on the continuity on interfaces between neighbouring elements. (For various applications of the DGFEM to compressible flow, see e. g. [1], [2], [3], [4], [11], [17]. Theory of the DGFEM applied to nonlinear nonstationary convection diffusion problems can be found in [5], [6] and [8].) The discontinuous Galerkin space semidiscretization is combined with a semi-implicit time discretization and a special treatment of boundary conditions in inviscid convective terms. In this way we obtain a numerical scheme requiring the solution of only one linear system on each time level.

The computational results show that the presented method is applicable to the numerical solution of inviscid compressible high-speed flow as well as flow with a very low Mach number at incompressible limit.

2 CONTINUOUS PROBLEM

For simplicity of the treatment we shall consider two-dimensional flow, but the method can be applied to 3D flow as well. The system of the Euler equations describing 2D inviscid flow can be written in the form

$$\frac{\partial \boldsymbol{w}}{\partial t} + \sum_{s=1}^{2} \frac{\partial \boldsymbol{f}_s(\boldsymbol{w})}{\partial x_s} = 0 \quad \text{in } Q_T = \Omega \times (0,T), \tag{1}$$

where $\Omega \subset \mathbb{R}^2$ is a bounded domain occupied by gas, $T > 0$ is the length of a time interval,

$$\boldsymbol{w} = (w_1, \dots, w_4)^{\mathrm{T}} = (\rho,\, \rho v_1,\, \rho v_2,\, E)^{\mathrm{T}} \tag{2}$$

is the so-called state vector and

$$\boldsymbol{f}_s(\boldsymbol{w}) = (\rho v_s,\, \rho v_s v_1 + \delta_{s1} p,\, \rho v_s v_2 + \delta_{s2} p,\, (E+p)\, v_s)^{\mathrm{T}} \tag{3}$$

are the inviscid (Euler) fluxes of the quantity $\boldsymbol{w}$ in the directions x_s, $s = 1, 2$. We use the following notation: ρ – density, p – pressure, E – total energy, $\boldsymbol{v} = (v_1, v_2)$ – velocity, δ_{sk} – Kronecker symbol. The equation of state implies that

$$p = (\gamma - 1)\,(E - \rho|\boldsymbol{v}|^2/2). \tag{4}$$

Here $\gamma > 1$ is the Poisson adiabatic constant. The system (1) – (4) is *hyperbolic*. It is equipped with the initial condition

$$\boldsymbol{w}(\boldsymbol{x}, 0) = \boldsymbol{w}^0(x), \quad x \in \Omega, \tag{5}$$

and the boundary conditions, which are treated in Section 4. We define the matrix

$$\boldsymbol{P}(\boldsymbol{w}, \boldsymbol{n}) = \sum_{s=1}^{2} \boldsymbol{A}_s(\boldsymbol{w}) n_s, \tag{6}$$

where $\boldsymbol{n} = (n_1, n_2) \in I\!R^2,\ n_1^2 + n_2^2 = 1$ and

$$\boldsymbol{A}_s(\boldsymbol{w}) = \frac{D\boldsymbol{f}_s(\boldsymbol{w})}{D\boldsymbol{w}},\ s = 1, 2, \tag{7}$$

are the Jacobi matrices of the mappings $\boldsymbol{f}_s$. It is possible to show that $\boldsymbol{f}_s,\ s = 1, 2$, are homogeneous mappings of order one, which implies that

$$\boldsymbol{f}_s(\boldsymbol{w}) = \boldsymbol{A}_s(\boldsymbol{w})\boldsymbol{w},\ s = 1, 2. \tag{8}$$

3 DISCRETIZATION

3.1 Space discontinuous Galerkin discretization

Let Ω_h be a polygonal approximation of Ω. By $\mathcal{T}_h$ we denote a partition of Ω_h consisting of various types of convex elements $K_i \in \mathcal{T}_h,\ i \in I$ ($I \subset Z^+ = \{0, 1, 2, \ldots\}$ is a suitable index set), e. g., triangles, quadrilaterals or in general convex polygons. (Let us note that in [8] it was shown that in the DGFEM also general nonconvex star-shaped polygonal elements can be used.) By Γ_{ij} we denote a common edge between two neighbouring elements K_i and K_j. The symbol $\boldsymbol{n}_{ij} = ((n_{ij})_1, (n_{ij})_2)$ denotes the unit outer normal to ∂K_i on the side Γ_{ij}. Moreover, we set $s(i) = \{j \in I; K_j \text{ is a neighbour of } K_i\}$. The boundary $\partial\Omega_h$ is formed by a finite number of faces of elements K_i adjacent to $\partial\Omega_h$. We denote all these boundary faces by S_j, where $j \in I_b \subset Z^- = \{-1, -2, \ldots\}$. Now we set $\gamma(i) = \{j \in I_b; S_j \text{ is a face of } K_i \in \mathcal{T}_h\}$ and $\Gamma_{ij} = S_j$ for $K_i \in \mathcal{T}_h$ such that $S_j \subset \partial K_i,\ j \in I_b$. For K_i not containing any boundary face S_j we set $\gamma(i) = \emptyset$. Obviously, $s(i) \cap \gamma(i) = \emptyset$ for all $i \in I$. Now, if we write $S(i) = s(i) \cup \gamma(i)$, we have

$$\partial K_i = \bigcup_{j \in S(i)} \Gamma_{ij}, \quad \partial K_i \cap \partial\Omega_h = \bigcup_{j \in \gamma(i)} \Gamma_{ij}. \tag{9}$$

The approximate solution will be sought at each time instant t as an element of the finite-dimensional space

$$\begin{aligned} \boldsymbol{S}_h &= \boldsymbol{S}^{r,-1}(\Omega_h, \mathcal{T}_h) \\ &= \{v; v|_K \in P^r(K)\ \forall\, K \in \mathcal{T}_h\}^4, \end{aligned} \tag{10}$$

where $r \geq 0$ is an integer and $P^r(K)$ denotes the space of all polynomials on K of degree $\leq r$. Functions $\boldsymbol{\varphi} \in \boldsymbol{S}_h$ are in general discontinuous on interfaces Γ_{ij}. By $\boldsymbol{\varphi}|_{\Gamma_{ij}}$ and $\boldsymbol{\varphi}|_{\Gamma_{ji}}$ we denote the values of $\boldsymbol{\varphi}$ on Γ_{ij} considered from the interior and the exterior of K_i, respectively. The symbols

$$\langle\boldsymbol{\varphi}\rangle_{ij} = \frac{1}{2}\left(\boldsymbol{\varphi}|_{\Gamma_{ij}} + \boldsymbol{\varphi}|_{\Gamma_{ij}}\right), \quad [\boldsymbol{\varphi}]_{ij} = \boldsymbol{\varphi}|_{\Gamma_{ij}} - \boldsymbol{\varphi}|_{\Gamma_{ji}} \tag{11}$$

denote the average and jump of a function $\boldsymbol{\varphi}$ on $\Gamma_{ij} = \Gamma_{ji}$.

In order to derive the discrete problem, we multiply (1) by a test function $\boldsymbol{\varphi} \in \boldsymbol{S}_h$, integrate over any element K_i, $i \in I$, apply Green's theorem and sum over all $i \in I$. Then we approximate fluxes through the faces Γ_{ij} with the aid of a numerical flux $\boldsymbol{H} = \boldsymbol{H}(\boldsymbol{u}, \boldsymbol{w}, \boldsymbol{n})$ in the form

$$\begin{aligned} &\int_{\Gamma_{ij}} \sum_{s=1}^{2} \boldsymbol{f}_s(\boldsymbol{w}(t))\,(n_{ij})_s \cdot \boldsymbol{\varphi}\,\mathrm{d}S \\ &\approx \int_{\Gamma_{ij}} \boldsymbol{H}(\boldsymbol{w}_h(t)|_{\Gamma_{ij}}, \boldsymbol{w}_h(t)|_{\Gamma_{ji}}, \boldsymbol{n}_{ij}) \cdot \boldsymbol{\varphi}\,\mathrm{d}S. \end{aligned} \tag{12}$$

If we introduce the forms

$$\begin{aligned} (\boldsymbol{w}_h, \boldsymbol{\varphi}_h)_h &= \int_{\Omega_h} \boldsymbol{w}_h \cdot \boldsymbol{\varphi}_h\,\mathrm{d}\boldsymbol{x}, \\ \tilde{b}_h(\boldsymbol{w}_h, \boldsymbol{\varphi}_h) &= \sigma_1 + \sigma_2, \end{aligned} \tag{13}$$

where

$$\begin{aligned} \sigma_1 &= -\sum_{K \in \mathcal{T}_h} \int_K \sum_{s=1}^{2} \boldsymbol{f}_s(\boldsymbol{w}_h) \cdot \frac{\partial \boldsymbol{\varphi}_h}{\partial x_s}\,\mathrm{d}\boldsymbol{x}, \\ \sigma_2 &= \sum_{K_i \in \mathcal{T}_h} \sum_{j \in S(i)} \int_{\Gamma_{ij}} \boldsymbol{H}(\boldsymbol{w}_h|_{\Gamma_{ij}}, \boldsymbol{w}_h|_{\Gamma_{ji}}, \boldsymbol{n}_{ij}) \cdot \boldsymbol{\varphi}_h \mathrm{d}S, \end{aligned} \tag{14}$$

we can define an *approximate solution* of (1) as a function w_h satisfying the conditions

$$\begin{aligned} &\text{a)} \quad \boldsymbol{w}_h \in C^1([0,T]; \boldsymbol{S}_h), \\ &\text{b)} \quad \frac{\mathrm{d}}{\mathrm{d}t}(\boldsymbol{w}_h(t), \boldsymbol{\varphi}_h)_h + \tilde{b}_h(\boldsymbol{w}_h(t), \boldsymbol{\varphi}_h) = 0 \\ &\qquad \forall\, \boldsymbol{\varphi}_h \in \boldsymbol{S}_h\ \forall\, t \in (0,T), \\ &\text{c)} \quad \boldsymbol{w}_h(0) = \Pi_h \boldsymbol{w}^0, \end{aligned} \tag{15}$$

where $\Pi_h \boldsymbol{w}^0$ is the L^2-projection of $\boldsymbol{w}^0$ from the initial condition (5) on the space $\boldsymbol{S}_h$. If we set $r = 0$, then we obviously obtain the finite volume method.

Let us note that the numerical flux $\boldsymbol{H}$ is assumed to be (locally) Lipschitz-continuous, consistent, i. e.

$$\boldsymbol{H}(\boldsymbol{w}, \boldsymbol{w}, \boldsymbol{n}) = \sum_{s=1}^{2} \boldsymbol{f}_s(\boldsymbol{w}) n_s,$$

and conservative, i. e.

$$\boldsymbol{H}(\boldsymbol{u}, \boldsymbol{w}, \boldsymbol{n}) = -\boldsymbol{H}(\boldsymbol{w}, \boldsymbol{u}, -\boldsymbol{n}).$$

3.2 Time discretization

Relation (15), b) represents a system of ordinary differential equations which can be solved by a suitable numerical method. Usually, *Runge-Kutta schemes* are applied. However, they are conditionally stable and the time step is strongly limited by the CFL-stability condition. Another possibility is to use the fully implicit *backward Euler method*, but it leads to a large system of highly nonlinear algebraic equations whose numerical solution is rather complicated. Our aim is to obtain a higher order unconditionally stable scheme, which would require the solution of a linear system on each time level. This is carried out with the aid of a suitable partial linearization of the form $\tilde{b}_h$. In what follows, we consider a partition $0 = t_0 < t_1 < t_2 \dots$ of the time interval $(0, T)$ and set $\tau_k = t_{k+1} - t_k$. We use the symbol $\boldsymbol{w}_h^k$ for the approximation of $\boldsymbol{w}_h(t_k)$.

In [4] we described a new DG semi-implicit technique which is suitable for an efficient solution of inviscid stationary as well as nonstationary compressible flow. This technique is based on a linearization of the forms σ_1 and σ_2, defined by (14), and the use of the Vijayasundaram numerical flux (cf. [18] or [10], Section 3.3.4). In this way we obtain the form

$$\begin{aligned} b_h(\boldsymbol{w}_h^k, \boldsymbol{w}_h^{k+1}, \boldsymbol{\varphi}_h) \;=\; & -\sum_{K\in\mathcal{T}_h}\int_K \sum_{s=1}^{2} \boldsymbol{A}_s(\boldsymbol{w}_h^k(\boldsymbol{x}))\boldsymbol{w}_h^{k+1}(\boldsymbol{x})\cdot\frac{\partial\boldsymbol{\varphi}_h(\boldsymbol{x})}{\partial x_s}\,\mathrm{d}\boldsymbol{x} \\ & + \sum_{K_i\in\mathcal{T}_h}\sum_{j\in S(i)}\int_{\Gamma_{ij}} \big[\boldsymbol{P}^+\left(\langle\boldsymbol{w}_h^k\rangle_{ij}, \boldsymbol{n}_{ij}\right)\boldsymbol{w}_h^{k+1}|_{\Gamma_{ij}} \\ & + \boldsymbol{P}^-\left(\langle\boldsymbol{w}_h^k\rangle_{ij}, \boldsymbol{n}_{ij}\right)\boldsymbol{w}_h^{k+1}|_{\Gamma_{ji}}\big]\cdot\boldsymbol{\varphi}_h \mathrm{d}S, \end{aligned}$$

which is linear with respect to the second argument $\boldsymbol{w}_h^{k+1}$ and third argument $\boldsymbol{\varphi}_h$. Here, $\boldsymbol{P}^\pm = \boldsymbol{P}^\pm(\boldsymbol{w}, \boldsymbol{n})$ represents the positive/negative part of the matrix $\boldsymbol{P}$ defined on the basis of its diagonalization (see, e.g. [10], Section 3.1):

$$\boldsymbol{P} = \boldsymbol{T}\boldsymbol{D}\boldsymbol{T}^{-1},\ \boldsymbol{D} = \mathrm{diag}\,(\lambda_1, \dots, \lambda_4), \tag{16}$$

where $\lambda_1, \dots, \lambda_4$ are the eigenvalues of $\boldsymbol{P}$. Then we set

$$\begin{aligned} \boldsymbol{D}^\pm &= \mathrm{diag}\,(\lambda_1^\pm, \dots, \lambda_4^\pm), \\ \boldsymbol{P}^\pm &= \boldsymbol{T}\boldsymbol{D}^\pm\boldsymbol{T}^{-1}, \end{aligned} \tag{17}$$

where $\lambda^+ = \max\{a, 0\}$ and $\lambda^- = \min\{a, 0\}$.

On the basis of the above considerations we obtain the following semi-implicit scheme: For each $k \geq 0$ find $\boldsymbol{w}_h^{k+1}$ such that

$$\begin{aligned} &\text{a)}\ \ \boldsymbol{w}_h^{k+1} \in \boldsymbol{S}_h, \\ &\text{b)}\ \ \left(\frac{\boldsymbol{w}_h^{k+1} - \boldsymbol{w}_h^k}{\tau_k}, \boldsymbol{\varphi}_h\right)_h + b_h(\boldsymbol{w}_h^k, \boldsymbol{w}_h^{k+1}, \boldsymbol{\varphi}_h) = 0 \\ &\qquad\qquad \forall\,\boldsymbol{\varphi}_h \in \boldsymbol{S}_h,\ k = 0, 1, \dots, \\ &\text{c)}\ \ \boldsymbol{w}_h^0 = \Pi_h\boldsymbol{w}^0. \end{aligned} \tag{18}$$

This is a first order accurate scheme in time. In the solution of nonstationary flows, it is necessary to apply a scheme, which is sufficiently accurate in space as well as in time. One possibility is to apply the following two step second order time discretization: The use of (16), the second order approximation $\tilde{\boldsymbol{w}}_h^{k+1}$ of $\boldsymbol{w}_h(t_{k+1})$ obtained with the aid of extrapolation,

$$\tilde{\boldsymbol{w}}_h^{k+1} = \frac{\tau_k + \tau_{k-1}}{\tau_{k-1}} \boldsymbol{w}_h^k - \frac{\tau_k}{\tau_{k-1}} \boldsymbol{w}_h^{k-1}, \tag{19}$$

which replaces the state $\boldsymbol{w}_h^k$ in the form b_h, and the second order backward difference approximation of the time derivative of the solution at time t_{k+1} yield the following *two-step second-order scheme*: For each $k \geq 1$ find $\boldsymbol{w}_h^{k+1}$ such that

$$\begin{aligned}
&\text{a)} \quad \boldsymbol{w}_h^{k+1} \in \boldsymbol{S}_h, \qquad (20)\\
&\text{b)} \quad \frac{2\tau_k + \tau_{k-1}}{\tau_k(\tau_k + \tau_{k-1})} \left(\boldsymbol{w}_h^{k+1}, \boldsymbol{\varphi}_h\right)_h \\
&\qquad + b_h(\tilde{\boldsymbol{w}}_h^{k+1}, \boldsymbol{w}_h^{k+1}, \boldsymbol{\varphi}_h) \\
&\qquad = \frac{\tau_k + \tau_{k-1}}{\tau_k \tau_{k-1}} \left(\boldsymbol{w}_h^k, \boldsymbol{\varphi}_h\right)_h - \frac{\tau_k (\boldsymbol{w}_h^{k-1}, \boldsymbol{\varphi}_h)_h}{\tau_{k-1}(\tau_k + \tau_{k-1})} \\
&\qquad\qquad \forall\, \boldsymbol{\varphi}_h \in \boldsymbol{S}_h,\ k = 0, 1, \ldots, \\
&\text{c)} \quad \boldsymbol{w}_h^0 = \Pi_h \boldsymbol{w}^0, \\
&\qquad \boldsymbol{w}_h^1 \text{ obtained by the Runge-Kutta method.}
\end{aligned}$$

The linear algebraic system equivalent to (18), b) or (20), b) is solved by the GMRES method with a block diagonal preconditioning. In order to guarantee the stability of the scheme, we use the CFL condition

$$\tau_k \max_{K_i \in \mathcal{T}_h} \frac{1}{|K_i|} \left(\max_{j \in S(i)} |\Gamma_{ij}| \lambda^{\max}_{\boldsymbol{P}(\boldsymbol{w}_h^k|_{\Gamma_{ij}}, \boldsymbol{n}_{ij})} \right) \leq \text{ CFL}, \tag{21}$$

where $|K_i|$ denotes the area of K_i, $|\Gamma_{ij}|$ the length of the edge Γ_{ij}, CFL a given constant and $\lambda^{\max}_{\boldsymbol{P}(\boldsymbol{w}_h^k|_{\Gamma_{ij}}, \boldsymbol{n}_{ij})}$ is the maximal eigenvalue of the matrix $\boldsymbol{P}(\boldsymbol{w}_h^k|_{\Gamma_{ij}}, \boldsymbol{n}_{ij})$ defined by (6), where the maximum is taken over Γ_{ij}. Numerical experiments show that the CFL number can be practically unlimited.

4 BOUNDARY CONDITIONS

If $\Gamma_{ij} \subset \partial\Omega_h$, i.e. $j \in \gamma(i)$, it is necessary to specify the boundary state $\boldsymbol{w}|_{\Gamma_{ji}}$ appearing in the numerical flux $\boldsymbol{H}$ in the definition of the inviscid form b_h. The appropriate treatment of boundary conditions plays a crucial role in the solution of low Mach number flows.

On a fixed impermeable wall we employ a standard approach using the condition $\boldsymbol{v} \cdot \boldsymbol{n} = 0$ and extrapolating the pressure. On the inlet and outlet it is necessary to use

nonreflecting boundary conditions transparent for acoustic effects coming from inside of Ω. Therefore, *characteristics based* boundary conditions are used.

Using the rotational invariance, we transform the Euler equations to the coordinates $\tilde{x}_1$, parallel with the normal direction $\boldsymbol{n}_{ij}$ to the boundary, and $\tilde{x}_2$, tangential to the boundary, neglect the derivative with respect to $\tilde{x}_2$ and linearize the system around the state $\boldsymbol{q}_{ij} = \boldsymbol{Q}(\boldsymbol{n}_{ij})\boldsymbol{w}|_{\Gamma_{ij}}$, where

$$\boldsymbol{Q}(\boldsymbol{n}_{ij}) = \begin{pmatrix} 1, & 0, & 0, & 0 \\ 0, & (n_{ij})_1, & (n_{ij})_2, & 0 \\ 0, & -(n_{ij})_2, & (n_{ij})_1, & 0 \\ 0, & 0, & 0, & 1 \end{pmatrix} \tag{22}$$

is the rotational matrix. Then we obtain the linear system

$$\frac{\partial \boldsymbol{q}}{\partial t} + \boldsymbol{A}_1(\boldsymbol{q}_{ij})\frac{\partial \boldsymbol{q}}{\partial \tilde{x}_1} = 0, \tag{23}$$

for the transformed vector-valued function $\boldsymbol{q} = \boldsymbol{Q}(\boldsymbol{n}_{ij})\boldsymbol{w}$, considered in the set $(-\infty, 0) \times (0, \infty)$ and equipped with the initial and boundary conditions

$$\begin{aligned} &\boldsymbol{q}(\tilde{x}_1, 0) = \boldsymbol{q}_{ij}, \quad \tilde{x}_1 \in (-\infty, 0), \\ &\boldsymbol{q}(0, t) = \boldsymbol{q}_{ji}, \quad t > 0. \end{aligned} \tag{24}$$

The goal is to choose $\boldsymbol{q}_{ji}$ in such a way that this initial-boundary value problem is well posed, i.e. has a unique solution. The method of characteristics leads to the following process:

Let us put $\boldsymbol{q}^*_{ji} = \boldsymbol{Q}(\boldsymbol{n}_{ij})\boldsymbol{w}^*_{ji}$, where $\boldsymbol{w}^*_{ji}$ is a prescribed boundary state at the inlet or outlet. We calculate the eigenvectors $\boldsymbol{r}_s$ corresponding to the eigenvalues λ_s, $s = 1, \ldots, 4$, of the matrix $\boldsymbol{A}_1(\boldsymbol{q}_{ij})$, arrange them as columns in the matrix $\boldsymbol{T}$ and calculate $\boldsymbol{T}^{-1}$ (explicit formulae can be found in [10], Section 3.1). Now we set

$$\boldsymbol{\alpha} = \boldsymbol{T}^{-1}\boldsymbol{q}_{ij}, \quad \boldsymbol{\beta} = \boldsymbol{T}^{-1}\boldsymbol{q}^*_{ji}. \tag{25}$$

and define the state $\boldsymbol{q}_{ji}$ by the relations

$$\boldsymbol{q}_{ji} := \sum_{s=1}^{4} \gamma_s \boldsymbol{r}_s, \quad \gamma_s = \begin{cases} \alpha_s, & \lambda_s \geq 0, \\ \beta_s, & \lambda_s < 0. \end{cases} \tag{26}$$

Finally, the sought boundary state $\boldsymbol{w}|_{\Gamma_{ji}}$ is defined as

$$\boldsymbol{w}|_{\Gamma_{ji}} = \boldsymbol{w}_{ji} = \boldsymbol{Q}^{-1}(\boldsymbol{n}_{ij})\boldsymbol{q}_{ji}. \tag{27}$$

5 SHOCK CAPTURING

For high speed flows with shock waves and contact discontinuities it is necessary to avoid the Gibbs phenomenon manifested by spurious overshoots and undershoots in computed quantities near discontinuities and steep gradients. These phenomena do not occur in low Mach number regimes, however in the transonic case they cause instabilities in the semi-implicit solution. We present here one possibility, how to treat this problem.

The limiting technique is motivated by the paper [12], on the basis of which the left-hand side of (18), b) and (20), b) is augmented by the form β_{h1} defined by

$$\beta_{h1}(\boldsymbol{w}_h^k, \boldsymbol{w}_h^{k+1}, \boldsymbol{\varphi}) = C_1 \sum_{i\in I} h_{K_i}^{2-\delta} f(res_{K_i}^k) \int_{K_i} \nabla \boldsymbol{w}_h^{k+1} \cdot \nabla \boldsymbol{\varphi} \,\mathrm{d}\boldsymbol{x}, \tag{28}$$

where $C_1 \approx 1,\ \delta \in (0, 1/2)$,

$$f(\xi) = \frac{\xi}{1+\xi}, \quad \xi \geq 0, \tag{29}$$

and

$$res_K^k = \frac{1}{|K|} \int_K \left| \frac{(w_h^k)_1 - (w_h^{k-1})_1}{\tau_{k-1}} + \frac{\partial (w_h^k)_2}{\partial x_1} + \frac{\partial (w_h^k)_3}{\partial x_2} \right| \mathrm{d}\boldsymbol{x}. \tag{30}$$

Obviously, res_K^k measures the residual in the continuity equation and serves as a discontinuity indicator. However, the artificial viscosity terms are nonzero even in regions, where the exact solution is regular, which could lead to a small nonphysical entropy production in these regions. Therefore, we combine this technique with the approach proposed in [7]. It is based on the discontinuity indicator $g(i)$ defined by

$$g^k(i) = \int_{\partial K_i} [\rho_h^k]^2 \,\mathrm{d}S \big/ (h_{K_i} |K_i|^{3/4}), \quad K_i \in \mathcal{T}_h, \tag{31}$$

in the 2D case. (By $[\rho_h^k]$ we denote the jump of the density on ∂K_i at time t_k.) We define a discrete shock indicator on the basis of (31):

$$G^k(i) = 0, \quad \text{if } g^k(i) < 1, \quad G^k(i) = 1, \quad \text{if } g^k(i) \geq 1, \quad K_i \in \mathcal{T}_h. \tag{32}$$

Now, to the left-hand side of (18), b) and (20), b) we add the artificial viscosity form

$$\beta_{h2}(\boldsymbol{w}_h^k, \boldsymbol{w}_h^{k+1}, \boldsymbol{\varphi}) = \nu_1 \sum_{i\in I} h_{K_i} G^k(i) \int_{K_i} \nabla \boldsymbol{w}_h^{k+1} \cdot \nabla \boldsymbol{\varphi} \,\mathrm{d}\boldsymbol{x} \tag{33}$$

with $\nu_1 \approx 1$. Moreover, we propose to augment the left-hand side of (18), b) and (20), b) by adding the form

$$J_h(\boldsymbol{w}_h^k, \boldsymbol{w}_h^{k+1}, \boldsymbol{\varphi}) = \nu_2 \sum_{i\in I} \sum_{j\in s(i)} \frac{1}{2}\big(G^k(i) + G^k(j)\big) \int_{\Gamma_{ij}} [\boldsymbol{w}_h^{k+1}] \cdot [\boldsymbol{\varphi}] \,\mathrm{d}\mathcal{S}, \tag{34}$$

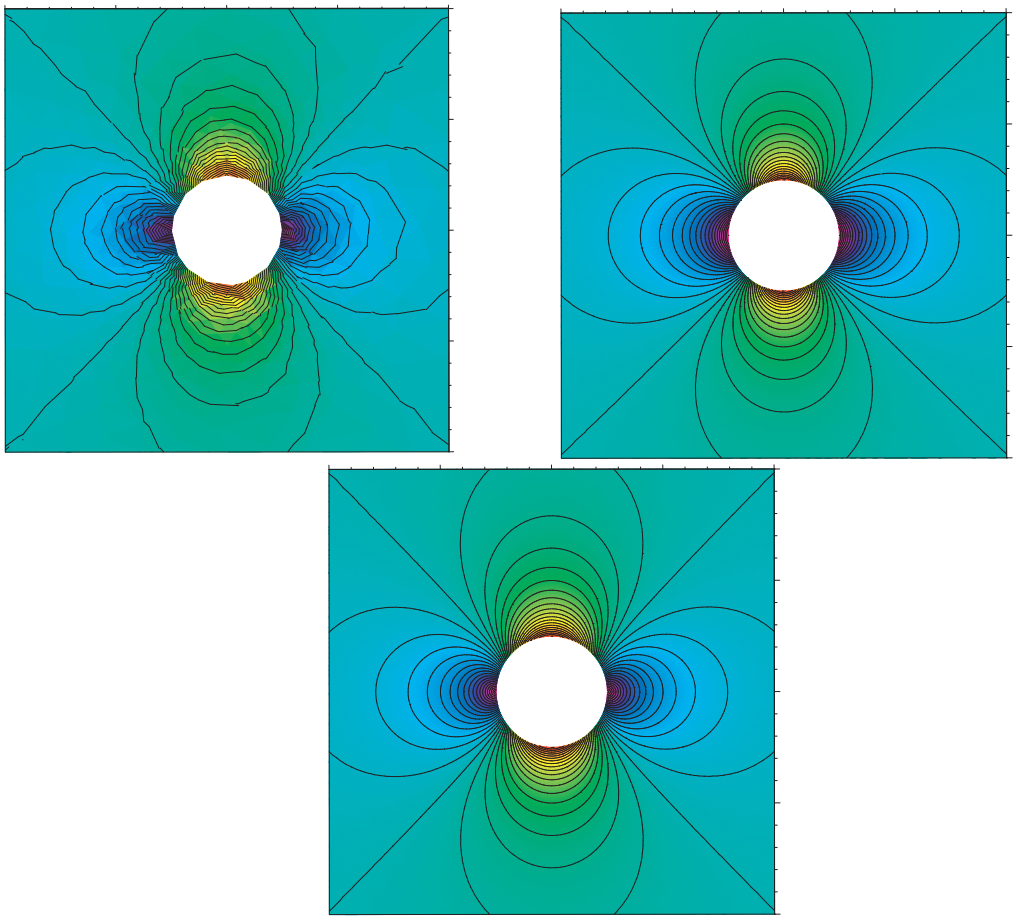

Figure 1: Velocity isolines for the approximate solution of compressible flow – coarse mesh (upper left), fine mesh (upper right), compared with the exact solution of incompressible flow (lower)

where $\nu_2 \approx 1$.

Thus, the resulting scheme obtained by limiting of (18), b) reads:

$$\begin{aligned}
&\text{a)} \quad \boldsymbol{w}_h^{k+1} \in \boldsymbol{S}_h, \qquad (35)\\
&\text{b)} \quad \left(\frac{\boldsymbol{w}_h^{k+1} - \boldsymbol{w}_h^k}{\tau_k}, \boldsymbol{\varphi}_h\right)_h + b_h(\boldsymbol{w}_h^k, \boldsymbol{w}_h^{k+1}, \boldsymbol{\varphi}_h)\\
&\quad +\beta_{h2}(\boldsymbol{w}_h^k, \boldsymbol{w}_h^{k+1}, \boldsymbol{\varphi}_h) + J_h(\boldsymbol{w}_h^k, \boldsymbol{w}_h^{k+1}, \boldsymbol{\varphi}_h) = 0, \ \forall\, \boldsymbol{\varphi}_h \in \boldsymbol{S}_h, \ k = 0, 1, \ldots,\\
&\text{c)} \quad \boldsymbol{w}_h^0 = \Pi_h \boldsymbol{w}^0.
\end{aligned}$$

(Similarly we obtain a limited version of scheme (20).) This method successfully overcomes problems with the Gibbs phenomenon in the context of the semi-implicit scheme. It is important that $G^k(i)$ vanishes in regions, where the solution is regular. Therefore, the scheme does not produce any nonphysical entropy in these regions (See Figure 5).

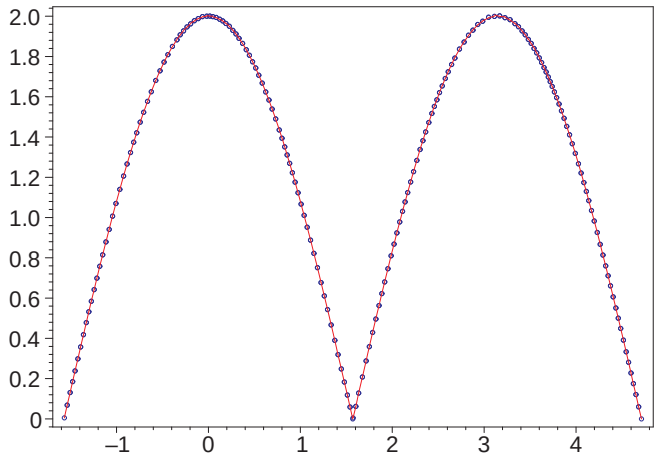

Figure 2: Velocity distribution along the cylinder (full line – compressible flow, dotted line – incompressible flow)

Remark 1 *In order to obtain an accurate, physically admissible solution, it is necessary to use isoparametric elements near curved boundaries (see [1] or [3]). In our computations we proceed in such a way that a reference triangle is transformed by a bilinear mapping on the approximation of a curved triangle adjacent to the boundary* $\partial\Omega$.

6 NUMERICAL EXAMPLES

In order to show the robustness of the described technique with respect to the Mach number, we present interesting results obtained by the semi-implicit scheme (35) for low Mach number flow as well as high speed transonic flow.

6.1 Low Mach number flow

First, let us consider stationary inviscid flow past a circular cylinder with the far field velocity parallel to the axis x_1 and the Mach number $M_\infty = 10^{-4}$. The problem was solved in a computational domain of the form of a square with sides of the length equal to 20 diameters of the cylinder. We show here details of the flow in the vicinity of the cylinder. Figure 1 shows isolines of the absolute value of the velocity for the compressible flow computed by scheme (35) with piecewise quadratic elements (i. e. $r = 2$), on a coarse mesh formed by 361 elements and on a fine mesh with 8790 elements, compared with the exact solution of incompressible flow (computed by the method of complex functions – see [9], Section 2.2.35). The steady-state solution was obtained with the aid of the time stabilization for "$t \to \infty$". In the case of the fine mesh the steady state was reached after 300 time steps, when the the L^∞-norm of the approximation of $\partial \boldsymbol{w}/\partial t$ was less than 10^{-8}.

$\#\mathcal{T}_h$	$\|error\|_{L^\infty(\Omega_h)}$	EOC
1251	5.05E-01	–
1941	4.23E-01	0.406
5031	2.77E-02	2.86
8719	6.68E-03	2.59

Table 1: Error in L^∞-norm and corresponding experimental order of convergence for the approximation of incompressible flow by low Mach number compressible flow with respect to $h \to 0$

The CFL number from the stability condition (21) was successively increased from 38 to 2000. This indicates that the method is practically unconditionally stable.

In Figure 2, the distribution of the absolute value of the velocity along the cylinder, computed on the fine mesh with 8790 elements, (related to the magnitude of the far field velocity) is shown. We see that the compressible and incompressible velocity distributions are identical.

Moreover, Table 1 presents the behaviour of the error and experimental order of convergence of the approximate solution $\boldsymbol{w}_h$ of compressible flow to the exact incompressible solution, measured in $L^\infty(\Omega_h)$-norm.

The maximum variation of the density $\rho_{\max} - \rho_{\min} = 2.3 \cdot 10^{-8}$, which corresponds to theoretical results (cf., e. g. [14]), and $\max_{K \in \mathcal{T}_h} |\nabla \rho_h|_K| < 1.99 \cdot 10^{-6}$. This indicates that the computed flow field behaves as incompressible flow.

In the second example we consider a compressible low Mach flow around the NACA 0012 profile. Figure 3 shows velocity isolines for the far field Mach number $M_\infty = 10^{-4}$ and zero angle of attack.

6.2 Transonic flow

The performance of shock capturing terms from Section 5 is tested on the GAMM channel with a 10% circular bump and the inlet Mach number equal to 0.67. The method (35) with piecewise quadratic elements (i.e. $r = 2$) is applied and the steady-state solution is obtained by the time stabilization for "$t \to \infty$". In this case a conspicuous shock wave is developed. In order to avoid the Gibbs phenomenon, manifested by spurious overshoots and undershoots near the shock wave, we tested the application of the artificial viscosity forms discussed in Section 5. Figures 4 and 5 show Mach number isolines and entropy isolines computed by scheme (35) using only locally artificial viscosity and penalization determined by forms β_{h2} and J_h from (33) and (34), respectively. One can see that scheme (35) yields the entropy production on the shock wave only, which is correct from the physical point of view.

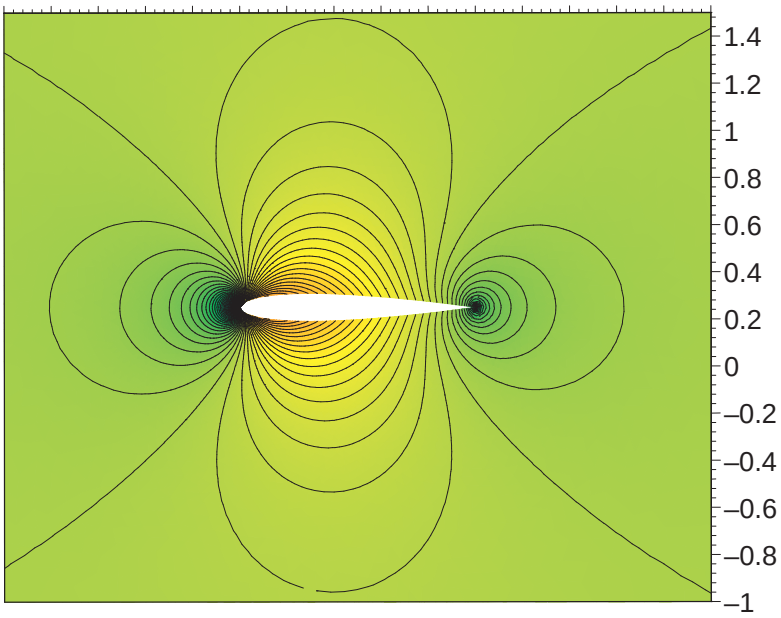

Figure 3: Velocity isolines around the NACA 0012 profile, $M_\infty = 10^{-4}$

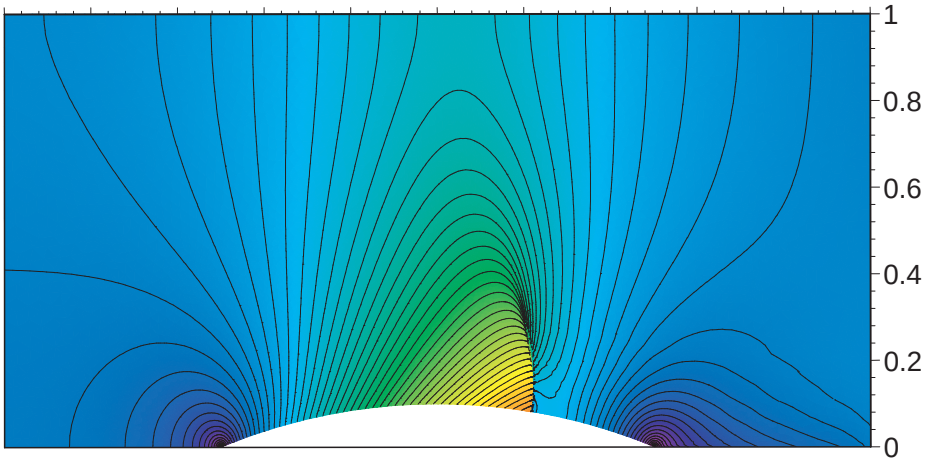

Figure 4: Transonic flow through the GAMM channel, Mach number isolines

7 CONCLUSION

In this paper we have presented a new method for the numerical solution of the Euler equations describing inviscid compressible flow. The method allows the simulation of

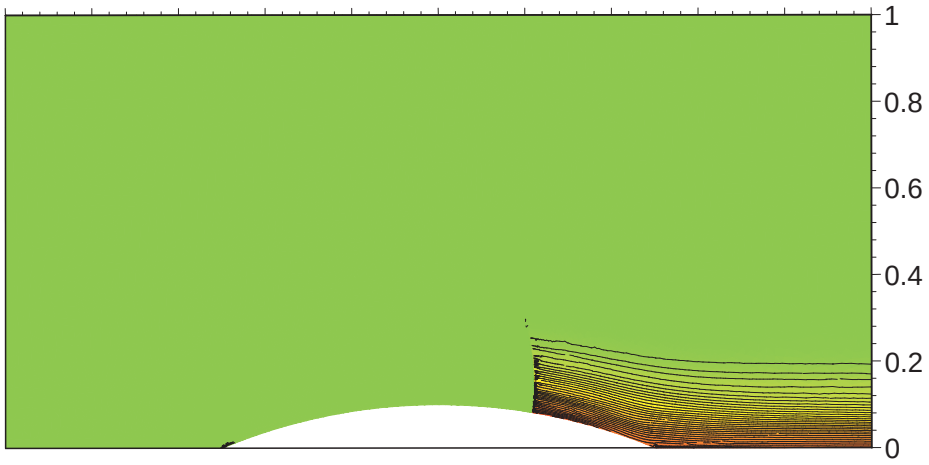

Figure 5: Transonic flow through the GAMM channel, entropy isolines

compressible flow with practically all Mach numbers – from very small values in the case of flows at incompressible limit, up to large Mach numbers for high speed transonic flows. There are several important ingredients making the method robust with respect to the Mach number, without the necessity to modify the Euler equations:

- discontinuous Galerkin space discretization,
- semi-implicit time discretization,
- characteristic treatment of boundary conditions,
- suitable limiting of order of accuracy in the vicinity of discontinuities in order to avoid the Gibbs phenomenon,
- the use of isoparametric finite elements at curved parts of the boundary.

Our further goal is the extension of the presented technique to compressible viscous flow described by the full system of the compressible Navier-Stokes equations.

Acknowledgements. This work is a part of the research project No. MSM 0021620839 of the Ministry of Education of the Czech Republic. The research of M. Feistauer was partly supported by the Grant No. 201/05/0005 of the Czech Grant Agency and the research of V. Kučera was partly supported by the Grant No. 6/2005/R of the Grant Agency of the Charles University. The authors acknowledge the support of these institutions.

REFERENCES

[1] F. Bassi and S. Rebay. High-order accurate discontinuous finite element solution of the 2D Euler equations. *J. Comput. Phys.*, **138**, 251–285, (1997).

[2] C. E. Baumann and J. T. Oden. A discontinuous *hp* finite element method for the Euler and Navier-Stokes equations. *Internat. J. Numer. Methods Fluids*, **31**, 79–95, (1999).

[3] V. Dolejší and M. Feistauer. On the discontinuous Galerkin method for the numerical solution of compressible high-speed flow. In F. Brezzi, A. Buffa, S. Corsaro, and A. Murli, editors, *Numerical Mathematics and Advanced Applications, ENUMATH 2001*, 65–84. Springer-Verlag Italia, (2003).

[4] V. Dolejší and M. Feistauer. A semi-implicit discontinuous Galerkin finite element method for the numerical solution of inviscid compressible flow. *J. Comput. Phys.*, **198**, 727-746, (2004).

[5] V. Dolejší and M. Feistauer. Error estimates of the discontinuous Galerkin method for nonlinear nonstationary convection-diffusion problems. *Numer. Func. Anal. Optimiz.*, **26**, 349-383, (2005).

[6] V. Dolejší, M. Feistauer and J. Hozman. Analysis of semi-implicit DGFEM for nonlinear convection-diffusion problems. *Comput. Methods Appl. Mech. Engrg.* (submitted). Preprint No. MATH-knm-2005/4, Charles University Prague, School of Mathematics (2005).

[7] V. Dolejší, M. Feistauer and C. Schwab. On some aspects of the discontinuous Galerkin finite element method for conservation laws. *Math. Comput. Simul.*, **61**, 333–346, (2003).

[8] V. Dolejší, M. Feistauer and V. Sobotíková. Analysis of the discontinuous Galerkin method for nonlinear convection–diffusion problems. *Comput. Methods Appl. Mech. Engrg.*, **194**, 2709–2733, (2005).

[9] M. Feistauer. *Mathematical Methods in Fluid Dynamics*. Longman Scientific & Technical, (1993).

[10] M. Feistauer, J. Felcman and I. Straškraba. *Mathematical and Computational Methods for Compressible Flow*. Clarendon Press, (2003).

[11] R. Hartmann and P. Houston. Goal oriented a posteriori error estimation for compressible fluid flows. In F. Brezzi, A. Buffa, S. Corsaro and A. Murli, editors, *Numerical Mathematics and Advanced Applications, ENUMATH 2001*, 775–784. Springer-Verlag Italia, (2003).

[12] J. Jaffre, C. Johnson and A. Szepessy. Convergence of the discontinuous Galerkin finite element method for hyperbolic conservation laws. *Math. Models Methods Appl. Sci*, **5**, 367-386, (1995).

[13] R. Klein. Semi-implicit extension of a Godunov-type scheme based on low Mach number asymptotics 1: one-dimensional flow. *J. Comput. Phys.*, **121**, 213–237, (1995).

[14] L. G. Loitsianskii: *Mechanics of Fluids and Gases*. Nauka, (1973) (in Russian).

[15] A. Meister and J. Struckmeier. *Hyperbolic Partial Differential Equations, Theory, Numerics and Applications*. Vieweg, (2002).

[16] S. Roller, C.-D. Munz, K. J. Geratz and R. Klein. The multiple pressure variables method for weakly compressible fluids. *Z. Angew. Math. Mech.* **77**, 481–484, (1997).

[17] J. J. W van der Vegt and H. Van der Ven. Space-time discontinuous Galerkin finite element method with dynamic grid motion for inviscid compressible flow, part I. General formulation. *J. Comput. Phys.*, **182**, 546–585, (2002).

[18] G. Vijayasundaram. Transonic flow simulation using upstream centered scheme of Godunov type in finite elements. *J. Comput. Phys.*, **63**, 416–433, (1986).

[19] P. Wesseling. *Principles of Computational Fluid Dynamics*. Springer, (2001).